Mechanism of Electrochemical Activity in Li_2MnO_3

Alastair D. Robertson and Peter G. Bruce*

School of Chemistry, University of St. Andrews, St. Andrews, Fife KY16 9ST, Scotland

Received February 19, 2003

Lithium intercalation compounds based on lithium manganese oxides are of great importance as positive electrodes for rechargeable lithium batteries. It is widely accepted that Li^+ may be extracted (deintercalated) from such lithium manganese oxides accompanied by oxidation of Mn up to a maximum oxidation state of +4. However, it has been suggested recently that further Li^+ removal may be possible. Among the mechanisms that have been proposed to charge balance the removal of Li^+ are Mn oxidation beyond +4 or loss of O^{2-}. To investigate this phenomenon we have selected Li_2MnO_3, a layered compound $Li[Li_{1/3}Mn_{2/3}]O_2$ with a ready supply of mobile Li^+ ions but with all Mn already in the +4 oxidation state. We show that a substantial quantity of Li (at least 1.39 Li) may be removed. At 55 °C this occurs exclusively by oxidation of the nonaqueous electrolyte, thus generating H^+ which exchange one-for-one with Li^+ to form $Li_{2-x}H_xMnO_3$. The presence of H^+ between the oxide layers results in a change of the layer stacking from O3 to P3, the latter being more stable for O−H−O bonding. At 30 °C initial Li removal is accompanied by oxygen loss (effective removal of Li_2O) but further Li^+ removal involves the same proton exchange mechanism as observed at 55 °C. The reaction is partially reversible. On extended cycling the material converts to spinel.

Introduction

Lithium intercalation compounds based on lithium manganese oxides are safer, cheaper, and less toxic than the intercalation compound $LiCoO_2$ and, therefore, offer a particularly attractive replacement for the latter compound as a positive electrode in rechargeable lithium batteries.[1,2] As a result, the lithium intercalation compound $LiMn_2O_4$ with the spinel structure, as well as orthorhombic and layered $LiMnO_2$ and their derivatives, have received intense interest in recent years.[3−8] Extraction of lithium from these compounds involves oxidation of Mn^{3+} to Mn^{4+}.

It is generally believed that Mn cannot be oxidized beyond +4 in an octahedral oxygen environment.[9] This limits the voltage of manganese-based cells because higher oxidation states correspond to d-levels lying at lower energy and hence higher electrode potentials. The inability to oxidize manganese beyond +4 also limits the amount of lithium that may be extracted from lithium manganese oxides, as removal of Li^+ is accompanied by oxidation of the Mn. This in turn limits the capacity of the cell to store charge. As a result, Mn^{4+} compounds such as Li_2MnO_3 (which adopts a layered structure $Li[Li_{1/3}Mn_{2/3}]O_2$), despite being rich in mobile Li^+ ions, were considered electrochemically inert. Recently, it has been suggested that Li^+ may be removed from Li−Mn^{4+}-oxides. For example, one report suggested the surprising result that lithium can be removed from Li_2MnO_3 by oxidation of Mn^{4+}.[10] Li_2MnO_3 is not the only compound which combines the presence of lithium ions with manganese in the +4 oxidation state. The nonstoichiometric spinel $Li_4Mn_5O_{12}$ ($Li[Li_{1/3}Mn_{5/3}]O_4$) is such a compound, as are the layered materials containing Mn^{4+}, Ni, and Li within the transition metal layers, e.g., $Li(Ni_xLi_{1/3-2x/3}Mn_{2/3-x/3})O_2$ ($0 \le x \le 1/3$).[11−13] It has been reported that lithium extraction is possible from these materials, not by oxidation of Mn^{4+} but by the simultaneous removal of oxygen to balance the charge; i.e., the effective removal of Li_2O.[14,15]

Clearly, the electrochemical activity of Li−Mn^{4+}-oxides is an interesting phenomenon and one for which contradictory explanations have been proposed. It has important implications for the use of lithium manganese oxides in rechargeable lithium batteries. As a result, it is important to investigate fundamentally whether Mn^{4+} may indeed be oxidized in an octahedral oxygen environment, or whether the removal of lithium is ac-

* Corresponding author. Fax: +44 1334 463825. E-mail: pgb1@st-and.ac.uk.

(1) Bruce, P. G. *J. Chem. Soc., Chem. Commun.* **1997**, 1817.
(2) Tarascon, J.-M.; Armand, M. *Nature* **2001**, *414*, 359.
(3) Thackeray, M. M.; David, W. I. F.; Bruce, P. G.; Goodenough, J. B. *Mater. Res. Bull.* **1983**, *18*, 461.
(4) Armstrong, A. R.; Bruce, P. G. *Nature* **1996**, *381*, 499.
(5) Wang, H.; Jang, Y.-I.; Chiang, Y.-M. *Electrochem. Solid State Lett.* **1999**, *2*, 490.
(6) Paulsen, J. M.; Dahn, J. R. *J. Electrochem. Soc.* **1999**, *146*, 3560.
(7) Robertson, A. D.; Armstrong, A. R.; Bruce, P. G. *J. Chem. Soc., Chem. Commun.* **2000**, 1997.
(8) Armstrong, A. R.; Paterson, A. J.; Robertson, A. D.; Bruce, P. G. *Chem. Mater.* **2002**, *14*, 710.
(9) See, for example, Ammundsen, B.; Paulsen, J. *Adv. Mater.* **2001**, *13*, 943.
(10) Kalyani, P.; Chitra, S.; Mohan, T.; Gopukumar, S. *J. Power Sources* **1999**, *80*, 103.
(11) Blasse, G.; *J. Inorg. Nucl. Chem.* **1963**, *25*, 743.
(12) Thackeray, M. M.; de Kock, A.; Russouw, M. H.; Liles, D. C.; Bittihn, R.; Hoge, D. *J. Electrochem. Soc.* **1992**, *139* 363.
(13) Lu, Z. ; MacNeil, D. D.; Dahn, J. R. *Electrochem. Solid State Lett.* **2001**, *4*, 191.
(14) Richard, M. N.; Fuller, E. W.; Dahn, J. R. *Solid State Ionics* **1994**, *73*, 81.
(15) Lu, Z.; Dahn, J. R. *J. Electrochem. Soc.* **2002**, *149*, 815.

10.1021/cm030047u CCC: $25.00
Published on Web 04/05/2003

companied by the extraction of oxygen, or does some other mechanism occur?

Li_2MnO_3 possesses a number of attractive features as a compound with which to investigate these issues. Being a layered structure, the Li^+ ions are expected to be mobile, and hence any limit on the ability to extract lithium by the conventional mechanism of transition metal oxidation is imposed by the Mn redox chemistry and not the availability of Li^+ ions on charging. A number of $Li-Mn^{4+}$-oxides contain other ions, especially transition metal ions such as Co and Ni. Li_2MnO_3 has the advantage, in the context of studying the fundamental mechanism of electrochemical activity in Mn^{4+} oxides, of being free from such complications. A brief communication reporting some unusual aspects of the behavior of Li_2MnO_3 has already been published by us.[16] However, here we extend the study to different temperatures and different degrees of charging. On charging at 55 °C, Li^+ in the Li_2MnO_3 electrode exchanges with H^+ generated by oxidation of the alkyl carbonate electrolyte at 4.5 V. At 30 °C, initial charging results in Li^+ removal for Li_2MnO_3 accompanied by oxygen loss from the oxide lattice. On further charging Li^+ exchanges for H^+ similar to the process at 55 °C.

Experimental Section

Stoichiometric Li_2MnO_3 was prepared by solid-state reaction between Li_2CO_3 (Aldrich, 99.5+%) and either $MnCO_3$ (Aldrich, 99.9+%) or electrolytic manganese dioxide (Sedema). Weights of starting materials were calculated to give 5 g of product. Powders were fired in air at a ramp rate of about 5 °C min^{-1} to a final temperature of either 500 °C for Li_2CO_3/ $MnCO_3$, or 800 °C for Li_2CO_3/ EMD, then quenched to room temperature. Reaction was complete in 40 h with an intermediate grinding.

Chemical analyses for lithium and manganese were carried out by flame emission and atomic absorption spectroscopy, respectively, using a Philips PU9400X AAS. The average manganese oxidation state was determined by redox titration using ferrous ammonium sulfate/$KMnO_4$.[17]

Powder X-ray diffraction data were collected on a Stoe STADI/P diffractometer operating in transmission mode with Fe $K\alpha_1$ radiation (λ = 1.936 Å). Manganese compounds fluoresce when irradiated with copper X-ray radiation. However, the use of an iron source coupled with a curved germanium monochromator and a small position-sensitive detector operating in transmission mode provides excellent data. Samples for ex-situ X-ray diffraction studies were prepared in the glovebox, and the sample holder was hermetically sealed to eliminate any reaction with the atmosphere during data collection.

Grain morphology and particle size were measured by scanning electron microscopy using a JEOL JSM-5600. Surface area measurements were carried out using the BET method by employing a Micormeritics Gemini 23670 instrument.

Electrochemical measurements were made using two electrode 2325 coin cells comprising a Li_2MnO_3 working electrode and Li metal counter electrode with a 1 molal solution of $LiPF_6$ in EC/DMC (1:1 v/v, Merck) as electrolyte. The Li_2MnO_3 electrodes were fabricated either as composite electrodes for extended galvanostatic cycling experiments or, more generally, as pressed pellets. The composite electrodes were formed by casting a mixture of the active material, acetylene black, and Kynar Flex 2801 binder in the weight ratios 75:17:8, onto Al foil using a fugitive solvent such as tetrahydrofuran. After the solvent had evaporated, the foils were cold pressed and cut into disks (1.3 cm diam.). The pressed pellets were prepared by mixing active material with graphite in the weight ratio 79:21 then cold pressing. The active materials, conductive additives, and kynar binder were all dried under vacuum at 70 °C overnight prior to use, and the composite electrodes were also dried at 70 °C under vacuum. Electrochemical measurements were carried out at 30 and 55 °C using a Biologic Macpile II. Charge−discharge curves of cells containing composite electrodes and pressed pellets were compared to ensure reproducibility. After cycling, cells were transferred to an argon-filled glovebox before opening, and active material was removed. The electrodes were then rinsed with a small amount of dry solvent to remove residual electrolyte. They were then left under dynamic vacuum overnight to ensure all solvent had evaporated.

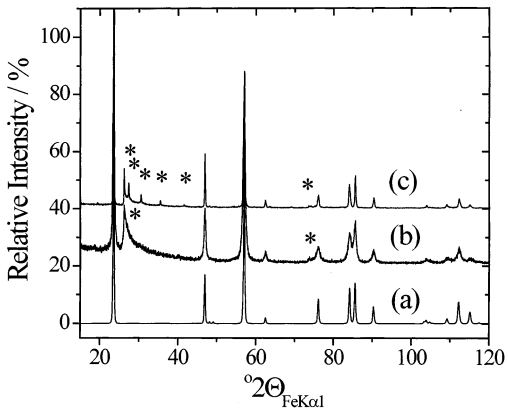

Figure 1. XRD patterns of Li_2MnO_3 (a) simulated pattern based on a rhombohedral unit cell, space group $R\bar{3}m$ a = 2.850 Å, c = 14.25 Å; (b) as-prepared material synthesized at 500 °C; and (c) as-prepared material synthesized at 800 °C. Note * = superstructure peaks.

Information on manganese oxidation state at various states of charge was also obtained from XPS measurements on as-cast, open circuit voltage, charged and discharged Li_2MnO_3 composite electrodes. Binding energies were charge-corrected using the C_{1s} peak (284.4 eV).

Combined thermogravimetric analysis/mass spectrometry (TGA−MS) measurements were performed using a Netzsch STA449 Jupiter instrument coupled with a Pfeiffer Vacuum Thermostar GSD300T. The TGA heating rate was 5 °C min^{-1} up to 400 °C under an argon atmosphere. Samples were transferred to the TGA−MS in gastight containers.

FTIR measurements on various Li_2MnO_3 electrodes were made from 400 to 4000 cm^{-1} with a Nicolet Avatar 360 using KBr (dried overnight at 300 °C) and active material. The KBr disks were prepared inside an argon filled glovebox and transferred to the spectrometer in a sealed glass vial prior to measurement to avoid contact with the atmosphere.

Results

Powder X-ray diffraction patterns for Li_2MnO_3 synthesized at 500 and 800 °C are shown in Figure 1. The peak widths at half-maximum are less for the material prepared at 800 °C as expected, however there are also additional peaks in the powder pattern of the material prepared at this higher temperature. The structure of Li_2MnO_3 consists of cubic close-packed oxide ions with alternate sheets of octahedral sites between the close-packed layers occupied by Li and $[Li_{1/3}Mn_{2/3}]$.[18] If the lithium and manganese ions in the transition metal layers are disordered then the structure is that of a simple layered compound with space group $R\bar{3}m$. It has

(16) Robertson, A. D.; Bruce, P. G. *J. Chem. Soc., Chem. Commun.* **2002**, 2790.

(17) Katz, M. J.; Clarke, R. C.; Nye, W. F. *Anal. Chem.* **1956**, *28*, 507.

(18) Strobel, P.; Lambert-Andron, B. *J. Solid State Chem.* **1998**, *75*, 90.

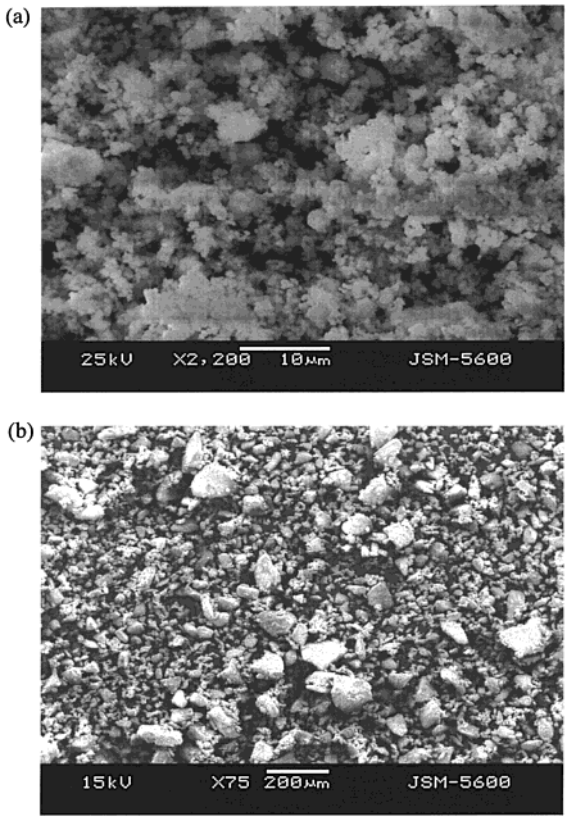

Figure 2. SEM images of as-prepared Li_2MnO_3 materials synthesized at (a) 500 °C and (b) 800 °C.

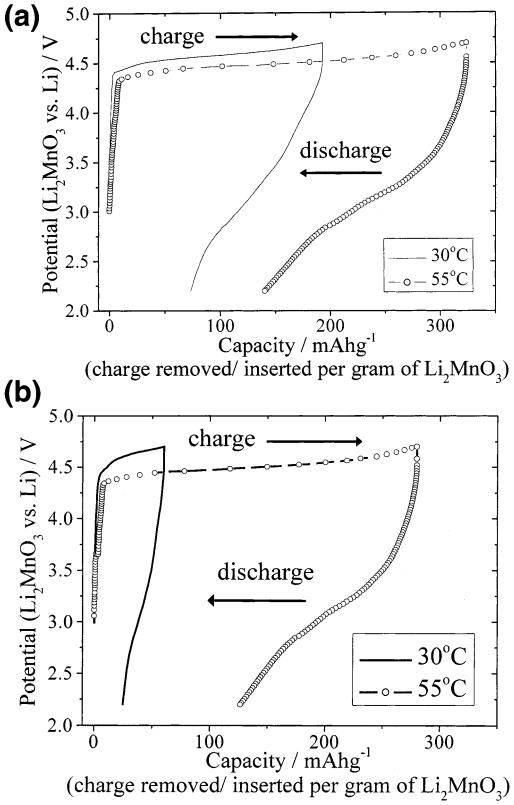

Figure 3. Variation of the cell potential (Li_2MnO_3 vs Li^+(1 M)/Li) on first charging then discharging the cells at 10 mAg^{-1} and at two different temperatures for Li_2MnO_3 prepared at (a) 500 °C and (b) 800 °C. Note that the charge capacity of the 800 °C material charged at 55 °C was 280 $mAhg^{-1}$ at a rate of 10 mAg^{-1}. This corresponds to a C-rate for the cell of C/28.

been suggested in the literature that the observed lowering in symmetry to *C*2/*m* is due to the ordering of Li and Mn ions in the transition metal layers. The powder pattern for the material prepared at 500 °C has many features reminiscent of a simple layered structure. There is, however, indication of some ordering of the lithium and manganese ions in the transition metal layer as demonstrated by the sawtooth peak at around 28° in 2θ. The material prepared at 800 °C has a higher degree of cation ordering as evident by the resolution of the sawtooth peak into two well-defined peaks, as shown in Figure 1.[19,20]

Scanning electron micrographs of the materials synthesized at 500 and 800 °C were collected and are shown in Figure 2. The greater particle size of the material prepared at 800 °C compared with that at 500 °C is evident. This is consistent with the results of surface area measurements by the BET method, which indicates surface areas of 3.7 m^2g^{-1} (500 °C) and 0.6 m^2g^{-1} (800 °C), and is also consistent with the narrower peak widths in the XRD patterns for the 800 °C material.

Behavior on the First Charge−Discharge Cycle. Cells were constructed using the 500 and 800 °C materials and cycled at a rate of 10 mAg^{-1} at 30 and 55 °C. The first charge and subsequent discharge curves for each cell are shown in Figure 3. Examining these figures there is no doubt that substantial charge may be removed from, and, to some extent, reinserted into, these cells. Qualitatively, the curves are similar, exhibiting a plateau at approximately 4.5 V on charging and then a steeply sloping curve on discharge. However, the quantity of charge removed and reinserted depends, to a significant extent, on the temperature used to synthesize the Li_2MnO_3 materials and the temperature at which the cells were cycled. By either cycling the cells at higher temperatures, or using smaller Li_2MnO_3 particles, substantially higher capacities are obtained suggesting a significant kinetic barrier to the electrochemical process. [It is important to note what is meant by the term capacity in the context of this paper. Fundamentally, capacity refers to the amount of charge that is extracted from, or inserted into, the cell per gram of Li_2MnO_3. Where this involves Li extraction from Li_2MnO_3 accompanied by oxygen loss, capacity also refers to the charge, and the amount of Li, removed from the material. When Li^+ removal is associated with H^+ exchange, capacity indicates the amount of Li^+ extracted and H^+ inserted in its place.] The relatively flat voltage curve on cycling could be indicative of a 2-phase deintercalation process associated with Li removed from Li_2MnO_3 or could indicate oxidation of the electrolyte.

To study the electrochemical reaction of Li_2MnO_3 accompanying charging of the cell in more detail, cells were charged to different degrees at 30 and 55 °C, then the electrodes were removed and investigated by various analytical methods including XPS, chemical analysis, and thermogravimetric analysis combined with mass spectrometry. The results of these measurements are presented in Tables 1 and 2 for the material prepared

(19) Russouw, M. H.; Thackeray, M. M. *Mater. Res. Bull.* **1991**, *26* 463.

(20) Tabuchi, M.; Nakashima, A.; Shigemura, H.; Ado, K.; Kobayashi, H.; Sakaebe, H.; Kageyama, H.; Nakamura, T.; Kohzaki, M.; Hirano, A.; Kanno, R. *J. Electrochem. Soc.* **2002**, *149*, 509.

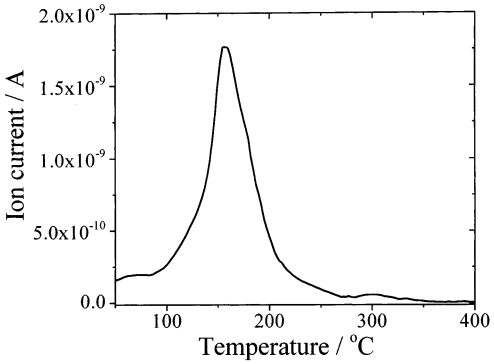

Figure 4. MS data for Li_2MnO_3-based material electrochemically delithiated at 55 °C indicating a mass 18 peak due to H_2O evolution on heating in the TGA−MS.

Table 1. Li_2MnO_3 XPS Binding Energy Results

sample[a]	Mn $2p_{3/2}$/eV	Mn $2p_{1/2}$/eV
As-cast Li_2MnO_3 composite electrode	642.7 (3.8)	654.1 (3.8)
OCV 55 °C 2 days	642.5 (4.4)	653.4 (5.0)
1st charge, 55 °C (Qc = 309 $mAhg^{-1}$)	642.4 (3.2)	653.7 (3.1)
1st charge, 30 °C (Qc = 235 $mAhg^{-1}$)	643.5 (3.6)	654.8 (3.6)
1st discharge, 55 °C (Qc = 309 $mAhg^{-1}$, Qd = 125 $mAhg^{-1}$)	642.4 (4.3)	653.1 (5.2)

[a] fwhm values in parentheses.

at 500 °C. Let us consider first the behavior at 55 °C. Up to 309 $mAhg^{-1}$ of charge was removed at 55 °C on the first charge, however, the XPS results are in agreement with a manganese oxidation state of +4 at the end of this process, Table 1.[21] Furthermore, there is no evidence in the XPS measurements for the oxidation of O^{2-}, something that might have been considered at these potentials (4.5 V vs Li^+(1M)/Li) given that such oxidation has been suggested in the literature.[22,23] It is clear from these results that the electrochemical reaction is not one of conventional deintercalation involving removal of Li^+ and e^-. The results of chemical analysis, Table 2, for the same electrode (309 $mAhg^{-1}$) indicate that the lithium content does, however, decrease on charging and that the amount of Li removed is in agreement with the quantity of charge extracted from the cell. Hence, lithium is clearly removed from the electrode despite the invariant Mn oxidation state. Does the electrochemical mechanism involve the simultaneous removal of oxide ions to balance the Li^+ that is extracted?

The electrode from which 309 $mAhg^{-1}$ of charge had been extracted at 55 °C was removed from the current collector, washed with dry solvent, and then dried under dynamic vacuum before being lightly ground. All these operations were carried out in an argon-filled glovebox. The sample was then transferred to the TGA−MS in a gastight container. The results of this analysis are presented in Figure 4. The electrode contained active material and carbon. The latter was expected to oxidize to CO and CO_2 on heating. Combining TGA with mass spectrometry is invaluable in this work as it permits identification of the different gases evolved (H_2O, CO, and CO_2) and separation of their weight losses. As a result it is possible to quantify the amount of H_2O, and hence H^+, in the material. Therefore, taking the XPS, chemical analysis, and TGA−MS results together for the electrodes charged to 309 $mAhg^{-1}$ at 55 °C, a composition for the charged material was derived and is reported in Table 2. It is evident that, upon charging, the cell lithium ions are removed from Li_2MnO_3 and replaced by protons. An electrode maintained at OCV for 48 h at 55 °C, washed, dried, and transferred to the TGA−MS in a fashion similar to that of the charged material, showed only a small amount of protons present in the material. This indicates that the H_2O in the charged material was unlikely to have arisen from, for example, decomposition of any residual electrolyte or from moisture entering the system in any other way. It is also apparent from Table 2 that the amount of protons present equals the amount of lithium removed. If the protons had arisen from any source other than ion exchange then this one-for-one correspondence would not have existed. There is no evidence for significant oxygen loss. The oxygen content of 2.95 should not be taken as indicating oxygen loss because it is close to 3, given the errors of the measurements.

A smaller amount of charge (199 $mAhg^{-1}$) was extracted from a cell at 55 °C and the lithium manganese oxide-based electrode was subjected to chemical and TGA−MS analysis (Table 2). Again, the quantity of Li removed from Li_2MnO_3 is in agreement with the charge passed. The extracted Li^+ is again replaced by an equal amount of H^+. There is no significant oxygen loss. We may conclude that at 55 °C the dominant mechanism of Li removal in Li_2MnO_3 involves exchange of Li^+ for H^+.

Considering now the behavior at 30 °C; the XPS results for the electrode from which 235 $mAhg^{-1}$ of charge was extracted indicates that Mn remains +4 and again there is no evidence of O^{2-} oxidation. Hence, a conventional mechanism of Li deintercalation can again be ruled out. As at 55 °C, the amount of Li removal on charge is in agreement with the charge passed. TGA−MS results indicate the presence of H^+ in the material, but unlike the behavior at 55 °C not all the Li^+ lost is replaced by H^+. As seen in Table 2 there is evidence of some oxygen deficiency. Approximately 60% of the Li removed is replaced by H^+, the rest being charge-compensated by oxygen loss. On extracting less charge (199 $mAhg^{-1}$) at 30 °C, it is evident from Table 2 that again two mechanisms of charge compensation, H^+ exchange and oxygen removal, operate. Despite removing less charge (199 instead of 235 $mAhg^{-1}$) the amount of oxygen lost is very similar. As a result, the proportion of Li removed that is balanced by H^+ exchange has dropped to around 45%. If only a small amount of charge is extracted (92 $mAhg^{-1}$) at 30 °C the mechanism is dominated by oxygen loss. It appears that, initially, on extracting Li during charging at 30 °C, oxygen is removed, however, as more Li is removed this mechanism of charge compensation gives way to H^+ exchange. We may conclude that both mechanisms operate at

(21) Eriksson, T.; Andersson, A. M.; Bishop, A. G.; Gejke, C.; Gustafsson, T.; Thomas, J. O. *J. Electrochem. Soc.* **2002**, *149*, 69.
(22) Aydinol, M. K.; Kohan, A. F.; Ceder, G.; Cho, K.; Joannopoulos, J. *Phys Rev. B* **1997**, *56*, 1354.
(23) Ohzuku, T.; Solid State Electrochemistry of Manganese (Di)-oxides for Advanced Lithium Batteries, presented at *IBA 2000 Manganese Oxide Symposium*, Chicago, IL, May 10−12, 2000.

Table 2. Analysis of Electrochemically Delithiated−Relithiated Li_2MnO_3 (FE, AAS, XPS, TGA−MS)

preparative conditions	observed composition Li:Mn ratio (FE/AAS)	theoretical Li:Mn ratio based on quantity of charge passed	avg. Mn valence (XPS)	H content (TGA−MS)	proposed bulk composition
OCV 55 °C, 48 h	$Li_{1.89}Mn_{1.00}$	$Li_{2.00}Mn_{1.00}$	4+	$H_{0.20}$	$Li_{1.89}H_{0.20}MnO_{3.04}$
1st charge, 55 °C −309 mAhg^{-1}	$Li_{0.62}Mn_{1.00}$	$Li_{0.65}Mn_{1.00}$	4+	$H_{1.29}$	$Li_{0.62}H_{1.29}MnO_{2.95}$
1st charge, 55 °C −199 mAhg^{-1}	$Li_{1.07}Mn_{1.00}$	$Li_{1.13}Mn_{1.00}$	4+	$H_{0.86}$	$Li_{1.07}H_{0.86}MnO_{2.97}$
1st charge, 30 °C −235 mAhg^{-1}	$Li_{0.87}Mn_{1.00}$	$Li_{0.97}Mn_{1.00}$	4+	$H_{0.64}$	$Li_{0.87}H_{0.64}MnO_{2.76}$
1st charge, 30 °C −199 mAhg^{-1}	$Li_{1.04}Mn_{1.00}$	$Li_{1.13}Mn_{1.00}$	4+	$H_{0.41}$	$Li_{1.04}H_{0.41}MnO_{2.73}$
1st charge, 30 °C −92 mAhg^{-1}	$Li_{1.63}Mn_{1.00}$	$Li_{1.60}Mn_{1.00}$	4+	$H_{0.14}$	$Li_{1.63}H_{0.14}MnO_{2.89}$
1st discharge, 55 °C −309 mAhg^{-1} then +125 mAhg $^{-1}$	$Li_{1.28}Mn_{1.00}$	$Li_{1.20}Mn_{1.00}$	4+	$H_{0.66}$	$Li_{1.28}H_{0.66}MnO_{2.97}$

30 °C but H^+ still dominates at high levels of Li extraction. The difference that raising the temperature has on the behavior is especially evident when comparing the two electrodes from which the same quantity of charge (199 mAhg^{-1}) was removed but at 30 and 55 °C respectively (Table 2). At the lower temperature oxygen loss and H^+ exchange occur, whereas at 55 °C only H^+ exchange occurs.

The results of XPS, chemical analysis, and TGA−MS on the 500 °C material after the first discharge at 55 °C are also presented in Tables 1 and 2. It is clear from Table 2 that upon discharge H^+ are removed and replaced by an equivalent amount of Li^+, however, not all the H^+ is removed. The process of replacing H^+ by Li^+ on the first discharge is clearly not fully reversible. The difficulty encountered in replacing protons by Li^+ ions on discharge is consistent with the rapidly decaying discharge potential (Figure 3). The XPS results reported in Table 1 for the 500 °C material charged then discharged at 55 °C indicate that Mn remains in the 4+ oxidation state throughout. The quantity of charge reinserted into the cell on discharge was calculated, and the composition derived based on replacing H^+ by Li^+ agrees well with the observed composition (Table 2); i.e., there is no evidence of a conventional intercalation mechanism involving Mn^{4+} reduction.

Two further techniques were employed to confirm the process of ion exchange and hence the presence of H^+ in the materials: infrared spectroscopy and magic angle spinning ^1H NMR. Infrared spectra were collected at the end of charge (−309 mAhg^{-1}) and discharge (−309 mAhg^{-1}, +125 mAhg^{-1}) for the cell operated at 55 °C (Figure 5). Also plotted in this figure are IR spectra for the as-prepared Li_2MnO_3 and the material left at open circuit for 48 h at 55 °C. All the materials were synthesized at 500 °C. Peak assignments are reported in Table 3 based on refs 24−30. All samples show low-

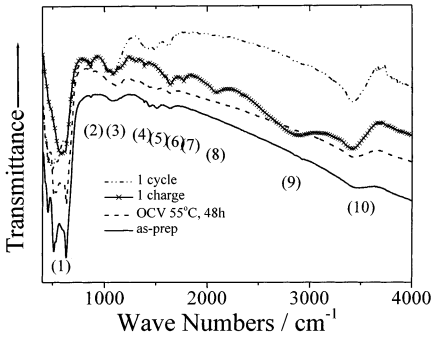

Figure 5. FTIR spectra of Li_2MnO_3-based samples.

Table 3. Occurrence and Assignments of Peaks in FTIR Spectra for Li_2MnO_3-based Materials[a]

peak	approximate frequency/cm^{-1}	proposed assignment
(1)	420−650	$[LiO_6]$, $[MnO_6]$
(2)	815−867	δ −OH, δ $-CO_3^{2-}$
(3)	1090 (b)	$[MnO_6]$, υ C═O
(4)	1383	δ −OH
(5)	1440, 1500 (db)	υ $-CO_3^{2-}$
(6)	1620−1645	δ −OH (H_2O)
(7)	1768 (b)	υ, υ_{as} C═O
(8)	2083	δ −OH
(9)	2700−3050 (b)	υ −OH
(10)	3500 (b)	υ −OH

[a] Key: b = broad, db = doublet, δ = bending mode, υ = stretch, υ_{as} = asymmetric stretch.

frequency bands at 420−650 cm^{-1} and 1090 cm^{-1} that arise from Li and Mn in octahedral coordination. The as-prepared material shows several small peaks at around 1400−1650 cm^{-1} and a peak at 3500 cm^{-1}. These peaks are associated with traces of carbonate (probably Li_2CO_3) and surface-adsorbed moisture. The −OH peaks are also present in KBr disks even in the absence of Li_2MnO_3. Interestingly, the spectrum of the material at OCV shows much less evidence of the peaks between 1400 and 1650 cm^{-1}. This suggests (a) that the Li_2CO_3 present on the surface of the as-prepared material prior to exposure to the electrolyte is removed in the electrolyte, and (b) that a surface layer is not generated by reaction with the electrolyte. Although containing Mn^{4+}, the OCV is ∼3 V (Figure 3) so that little electrolyte oxidation (and hence surface layer formation) is expected at OCV, as observed.

On charging, the peak at 3500 cm^{-1} associated with hydrogen bonded −OH grows significantly compared with that of the as-prepared material, then diminishes

(24) Farmer, V. C., Ed. *The Infrared Spectra of Minerals*. Mineralogical Society: London, 1974.
(25) Feng, Q.; Miyai, Y.; Kanoh, H.; Ooi, K. *Langmuir* **1992**, *8*, 1861.
(26) Ammundsen, B.; Aitchison, P. B.; Burns, G. R.; Jones, D. J.; Rozière, J. *Solid State Ionics* **1997**, *97*, 269.
(27) Kohler, T.; Armbruster, T.; Libowitzky, E. *J. Solid State Chem.* **1997**, *133*, 486.
(28) MacLean, L. A. H.; Tye, F. L. *J. Mater. Chem.* **2001**, *11*, 891.
(29) Du Pasquier, A.; Blyr, A.; Courjal, P.; Larcher, D.; Amatucci, G.; Gérand, B.; Tarascon, J. M. *J. Electrochem. Soc.* **1999**, *146*, 428.
(30) Moshkovich, M.; Cojocaru, M.; Gottlieb, H. E.; Aurbach, D. *J. Electroanal. Chem.* **2001**, *497*, 84.

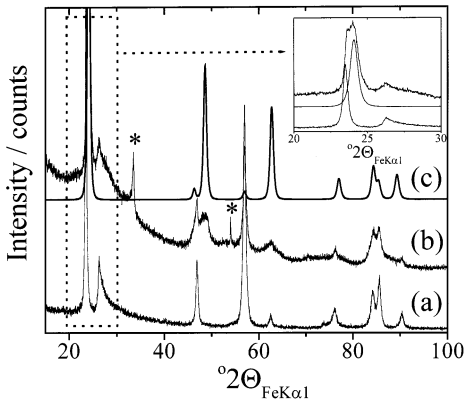

Figure 6. Powder X-ray diffraction data for (a) as-synthesized Li_2MnO_3; (b) Li_2MnO_3-based electrode after electrochemical extraction of 1.35 Li; and (c) simulated *P*3 pattern for a delithiated sample, space group $R3m$, $a = 2.885$ Å, $c = 13.91$ Å. Note * = graphite in (b).

somewhat on subsequent discharge. In addition, the charged sample shows a peak at 2083 cm^{-1} and a very broad peak observed in the region 2700−3050 cm^{-1}. These bands have been seen in several MnOOH compounds by previous authors and are associated with −OH bending and stretching modes, respectively.[27,28] The broad peak around 2700−3050 cm^{-1} is indicative of H-bonded −OH where the hydrogen bonding is stronger than is the case for the hydroxl groups whose stretching mode occurs around 3500 cm^{-1}. This suggests that ordering of hydroxyl groups occurs during exchange of H^+ with Li^+ in Li_2MnO_3. On subsequent discharge (relithiation) the peaks at 2083 and 2700−3050 cm^{-1} are no longer evident suggesting that the remaining hydroxl groups are less ordered. The remaining bands are consistent with other −OH modes, C═O, and C−C−O. The carbon-containing species arise from oxidation of the alkyl carbonate solvents[30] although the complexity of the spectra that arise from such decomposition prevents unambiguous assignment of individual bands to specific species.

Magic angle spinning ^1H NMR measurements were carried out using a 200 MHz CMXII spectrometer on the material charged at 55 °C by removal of 309 $mAhg^{-1}$. The results confirm the presence of protons in the sample, as evidenced by a peak at 299 ppm due to H-bonded protons. A more detailed analysis of the ^1H NMR of these materials will be described in a separate forthcoming publication.

Powder X-ray diffraction patterns were collected on the Li_2MnO_3 material from which 309 $mAhg^{-1}$ of charge was removed at 55 °C, and one such pattern is shown in Figure 6 along with a powder X-ray diffraction pattern for as-prepared Li_2MnO_3, for comparison. Although it is clear that there is a significant similarity between the two powder diffraction patterns, there are important differences. In view of the fact that the compound now contains a substantial quantity of protons, it is reasonable to consider whether structural features corresponding to that in known transition metal oxyhydroxides may have developed. In this regard we also present in Figure 6 a calculated powder pattern based on the P3 structure of CrOOH. This compound has a structure based on close-packed oxide ion layers stacked in an AABBCC sequence, with transition metal ions located between the AB, BC, and CA layers in the octahedral sites and protons in the interlayer space between adjacent oxide ion layers stacked in the same orientation i.e., AA, BB, CC.[31] The driving force for the adoption of this structure is the hydrogen bonding between adjacent oxide ion layers. The additional peaks present in the powder diffraction pattern for the exchanged material are consistent with this P3 structure indicating that at least a proportion of the material has undergone slippage of oxide ion layers to change the stacking sequence from O3 (ABC) to the P3 stacking (AABBCC). The peak at 49° 2θ is a particularly prominent example of one that is not present in Li_2MnO_3 but is characteristic of the P3 structure. The presence of strongly H-bonded −OH groups in the P3 phase is consistent with the broad peak in the FTIR spectrum at 2700−3050 cm^{-1} (Figure 5).

Behavior on Cycling. Cells constructed from Li_2MnO_3 prepared at 500 and 800 °C were cycled at a rate of 10 mAg^{-1} and at two temperatures, 30 and 55 °C. The charge−discharge curves for these cells are shown in Figures 7 and 8. Qualitatively, the evolution of these curves on cycling is similar. In all cases there is a significant difference between the first and subsequent cycles. This is especially so for the first and second charges. On the second charge the 4.5 V plateau is very small and by the third cycle it has disappeared. On cycling, there is a gradual development of 3 and 4 V plateaux. The 3 V plateau begins to become apparent even in the first discharge and is certainly well developed after 10 cycles in most cases. Such a voltage profile suggests the formation of spinel. To examine this in more detail, incremental capacity plots were constructed and are presented in Figure 9(a) for materials prepared at 500 and 800 °C and cycled at 55 °C. It is clear that after some 10 cycles the two pairs of redox peaks at around 4 V characteristic of spinel are present, whether the material was prepared at 500 or 800 °C. Confirmation is given in Figure 9(b) where the 4 V region is shown for Li_2MnO_3 after 50 cycles alongside Li_2MnO_4 spinel prepared by normal high-temperature solid-state synthesis, and layered Li_xMnO_2 after 25 cycles. The layered compound is known to transform to spinel on cycling.[8,32] The double 4 V process is evident in each case with a good match between the peak positions suggesting similar local structures for all three materials.

Although the qualitative features of the charge−discharge curves on cycling are similar for the 500 and 800 °C materials the kinetics do appear to be considerably different. This difference is apparent in Figure 10 where the variation of capacity with cycle number for electrodes synthesized at 500 and 800 °C is shown. The capacity for the 500 °C material actually rises within the first few cycles and then falls rapidly toward the development of a plateau. There is a much less pronounced rise in the case of the 800 °C material. Whereas the capacity of the 500 °C material is substantially higher than that of the 800 °C compound initially, the

(31) Christensen, A. N.; Hansen, P.; Lehmann, M. S. *J. Solid State Chem.* **1977**, *21*, 325.
(32) Robertson, A. D.; Armstrong, A. R.; Bruce, P. G. *Chem. Mater.* **2001**, *13*, 2380.

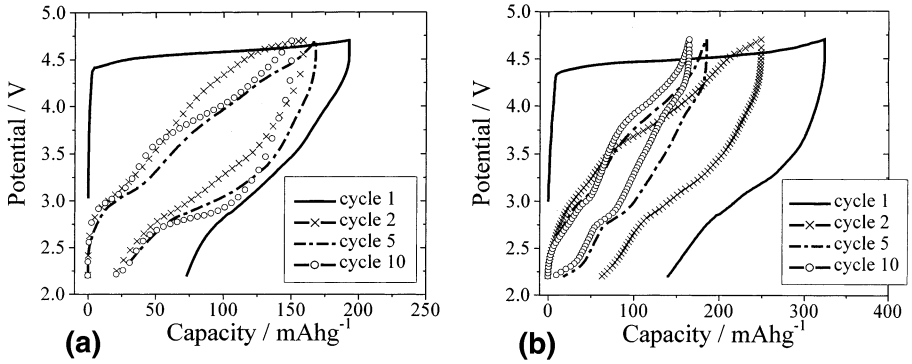

Figure 7. Charge−discharge curves for Li_2MnO_3-based electrode materials synthesized at 500 °C (a) at 30 °C and (b) 55 °C. Rate = 10 mAg^{-1}. Data have been normalized such that charging curves start at 0 $mAhg^{-1}$ for each selected cycle.

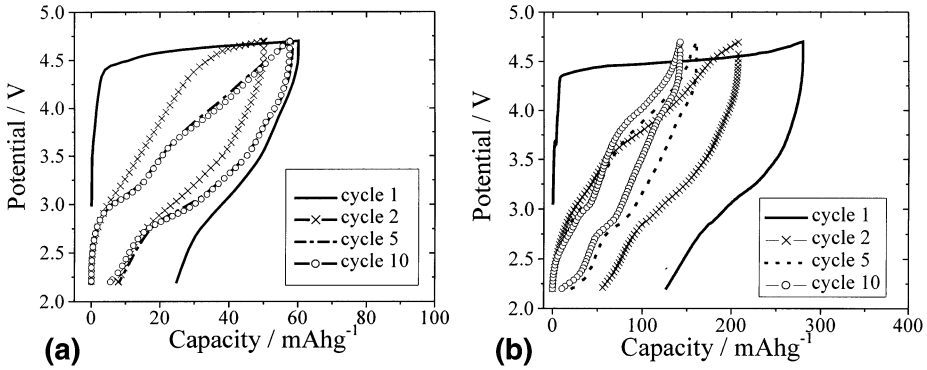

Figure 8. Charge−discharge curves for Li_2MnO_3-based electrode materials synthesized at 800 °C (a) at 30 °C and (b) 55 °C. Rate = 10 mAg^{-1}.

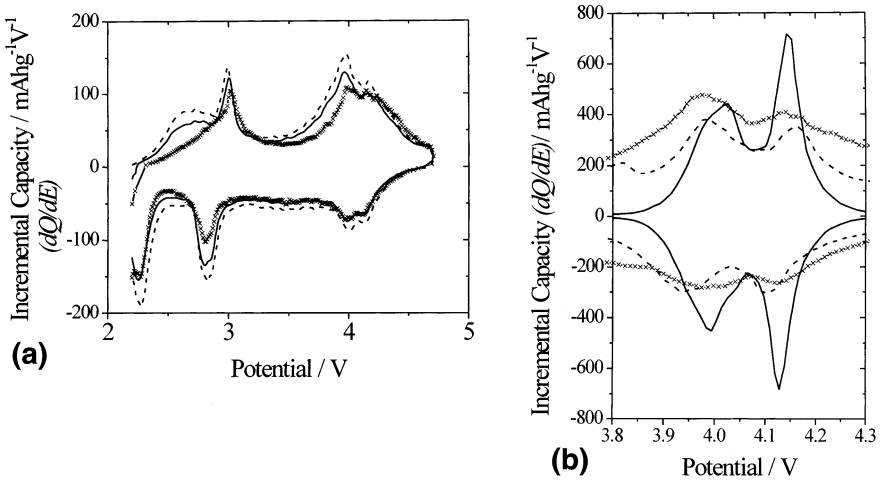

Figure 9. (a) Incremental capacity plots at 55 °C for Li_2MnO_3 prepared at 500 and 800 °C. Cycling was carried out at a rate of 10 mAg^{-1}. —— 500 °C, cycle 10; − − − 800 °C, cycle 10; —x— 500 °C, cycle 50. (b) Incremental capacity plots for three lithium manganese oxides cycled over a wide composition range. Rate = 10 mAg^{-1}. —— $LiMn_2O_4$ spinel; − − − Li_xMnO_2 cycle 25; —x— Li_2MnO_3 cycle 50.

capacities do converge at higher cycle numbers. The charge capacity exceeds that on discharge initially but here too the efficiency improves and approaches 100% at higher cycle numbers. The relative irreversibility between charge and discharge, as well as the significant dependence on particle size, are characteristic of the Li^+/H^+ exchange mechanism described above. It is, however, interesting that as the material evolves toward the spinel structure these features disappear. It would appear that regardless of the initial state of the materials they all evolve toward a material with a similar composition and structure, based on spinel.

Discussion

Early studies of Li_2MnO_3 in aqueous acidic media (H_2SO_4) were interpreted primarily in terms of the simultaneous removal of Li^+ and O^{2-} (Li_2O) forming MnO_2.[19,33] The authors reported a powder diffraction pattern similar to the one reported here in Figure 6 and interpreted it in terms of a P3 structure with the stacking sequence AABBCC. Such a stacking sequence may now, as stated above, be understood in terms of

(33) Russouw, M. H.; Liles, D. C.; Thackeray, M. M. *J. Solid State Chem.* **1993**, *104*, 464.

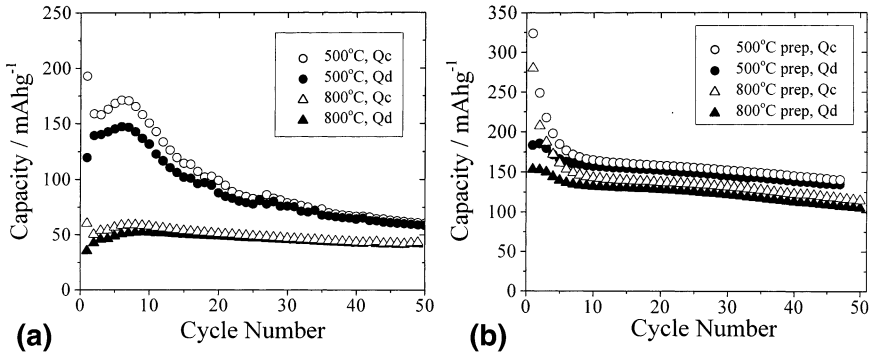

Figure 10. Cycling data for Li_2MnO_3-based electrode materials; Qc = charge capacity, Qd = discharge capacity. (a) $T = 30$ °C. (b) $T = 55$ °C. Rate = 10 mAg^{-1}.

the presence of protons, and hence hydrogen bonding in the structure. Very recently, the same group, in conjunction with co-workers at SUNY Stony Brook, have shown that in fact proton exchange rather than oxygen removal dominates the reaction of Li_2MnO_3 in aqueous acidic media.[32] The NMR studies clearly identify that the shearing of oxygen planes associated with the formation of P3 stacking is due to H-bonding. This is further discussed in their paper.[34] Tang et al. have also shown that under hydrothermal conditions the dominant process is exchange of Li^+ by H^+ at low proton concentrations, whereas oxygen loss, rather than ion exchange, occurs at high H^+ concentrations.[35] The significance of proton exchange in Mn^{4+} oxides has also been highlighted by Feng et al.[25] and Ammundsen et al.[26] in their studies of $Li_{1+x}Mn_{2-x}O_4$ ($0 \le x \le 0.33$) spinels in aqueous acidic media. They show that for $x = 0$ ($LiMn_2O_4$), in which 50% of the Mn is +3, lithium extraction occurs by Hunter's redox mechanism involving disproportionation of $2Mn^{3+}$ to Mn^{2+} and Mn^{4+}:

$$4LiMn^{3+}Mn^{4+}O_4 + 8H^+ \rightarrow 3Mn_2{}^{4+}O_4 + 4Li^+ + 2Mn^{2+} + 4H_2O$$

Whereas, for $x = 0.33$ ($Li_{1.33}Mn_{1.67}O_4 \equiv Li_4Mn_5O_{12}$), all the Mn is in the 4+ oxidation state and lithium extraction occurs by a proton exchange mechanism because no Mn^{3+} disproportionation and hence no Mn dissolution is possible:

$$3Li_{1.33}Mn^{4+}{}_{1.67}O_4 + 4H^+ \rightarrow 3Li_{1.33}Mn^{4+}{}_{1.67}O_4 + 4Li^+$$

At intermediate values of x, both redox and ion exchange reactions occur. The extent of each depends on the proportions of Mn^{3+} and Mn^{4+} in the original spinel material.

In contrast to all of these studies, the work reported here was carried out electrochemically in an anhydrous environment using nonaqueous electrolytes. However, fluorinated anions such as PF_6^- are notorious for the generation of some HF in the presence of even a small amount of H_2O. Du Pasquier et al., showed as part of a study of $LiMn_2O_4$ spinel electrodes in such fluorinated nonaqueous battery electrolytes, that the presence of H^+ leads to behavior reminiscent of aqueous acid solutions.[29] The protons promote disproportionation of Mn^{3+} at the surface of $LiMn_2O_4$ with dissolution of Mn^{2+} and formation of a Mn^{4+}-rich surface (essentially the Hunter mechanism described above). The Mn^{4+}-rich oxide surface then undergoes $Li^+ \leftrightarrow H^+$ ion exchange (essentially the Feng/Ammundsen mechanism described above). This latter process is similar to our observations for Li_2MnO_3 at open circuit. Since Li_2MnO_3 contains only Mn^{4+}, there is no disproportionation/Mn dissolution but H^+ exchanges slowly with Li^+. The extent is limited because of the limited concentration of H^+ in the electrolyte at the open circuit voltage of ~3 V. In the case of Du Pasquier et al.'s study, the lithium deficient spinel is at a potential of ~4.2 V (λ-MnO_2) which oxidizes the alkyl carbonates in the electrolyte generating significantly more H^+.

Turning now to the electrochemical behavior of Li_2MnO_3 on charging. The potential rises rapidly to 4.5 V, which places it below the top of the oxygen valence band. As such, we may anticipate oxidation of O^{2-} giving rise to evolution of oxygen at the electrode surface accompanied by two Li^+, i.e., the effective removal of Li_2O. It is unlikely that any oxidized O^{2-} species, e.g. O^- or O, would be stable for any length of time on the electrode surface so no such oxidized species is seen on removing the electrode and subjecting it to XPS. As shown by the results presented above, oxygen loss occurs to only a limited extent at 30 °C (and not at all at 55 °C) before being replaced by H^+ exchange. It is certainly possible that oxidized O^{2-} species, e.g. O^-, O etc., at the electrode surface play a role in oxidizing the electrolyte, even if they are short-lived, with the consequent generation of H^+. Changing the electrolyte to $LiBF_4$ in PC caused the potential of the plateau on charging to be reduced by 100 mV to 4.4 V reinforcing the effect of electrolyte stability against oxidation. It has been shown by a number of authors that potentials in excess of 4.2−4.5 V vs Li^+(1 M)/Li are sufficient to provide oxidation of alkyl carbonates resulting in the generation of H^+ at the electrode surface.[29,30,36,37] Therefore, despite the anhydrous nature of the electrolyte, protons can and do exist, especially near the electrode surface under oxidizing conditions. The H^+ thus generated then exchanges for Li^+ in the electrode. Oxidation of the electrolyte also supplies, of course, electrons to the external circuit. The processes on charging are

(34) Paik, Y.; Grey, C. P.; Johnson, C. S.; Kim, J.-S.; Thackeray, M. M. *Chem. Mater.* **2002**, *14* (12), 5106−5115.
(35) Tang, W.; Kanoh, H.; Yang, X.; Ooi, K. *Chem. Mater.* **2000**, *12*, 3271.
(36) Kanamura, K.; Toriyama, S.; Shiraishi, S.; Takehara, Z. *J. Electrochem. Soc.* **1996**, *143*, 2548.
(37) Kanamura, K. *J. Power Sources* **1999**, *81*−*82*, 123.

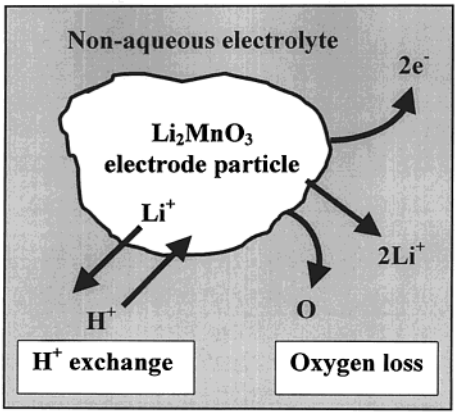

Figure 11. Schematic representation of processes occurring at the electrode/ electrolyte interface.

illustrated in Figure 11. Discharge involves reduction of the electrolyte with consumption of H^+ thus driving its removal from the electrode and replacement with Li^+.

Although it has been shown that alkyl carbonate based electrolytes can undergo oxidation at potentials in excess of 4.2 to 4.4 V vs Li^+(1 M)/ Li leading to H^+ generation:

$$R - H \rightarrow R^0 + H^+ + e^-$$

in reality the electrolyte oxidation mechanism is much more complex.[29,30,36,37] Aurbach and co-workers have in particular carried out detailed studies on the oxidation of alkyl carbonate-based electrolytes using a variety of techniques including FTIR, NMR, and MS.[30] They included in their study the electrolyte based on ethylene carbonate and dimethyl carbonate. Many decomposition products are identified. It is proposed that the cyclic carbonates such as EC are more reactive than their linear chain analogues.[30] In the case of EC, different reaction schemes for the oxidation of this molecule have been suggested. One possible reaction pathway[30] is the following:

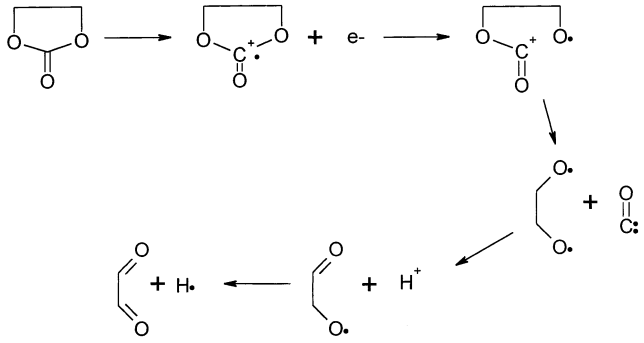

Although the details are not clear it is evident that solvents such as EC can and do undergo oxidation generating H^+.

Surface layers exist on many lithium transition metal oxides even before they are placed in contact with an electrolyte. The layer is typically rich in Li_2CO_3 or LiOH. In the case of Li_2MnO_3, contact with the nonaqueous electrolyte appears to deplete this layer (Figure 5 and description of FTIR results, above). It has been known for a number of years that surface layers can form on lithium transition metal oxides if the electrode potential is sufficiently high to oxidize the electrolyte.[38] This topic has received much interest recently with significant advances in understanding the layers, although the surface chemistries are not fully understood at present.[21,37,39,40] In the case of Li_2MnO_3 at OCV (~3 V) it appears surface layers do not form. However, FTIR data for the charged Li_2MnO_3 electrodes do show bands typical of the products of oxidation (Figure 5), although it was not possible to assign unambiguously these bands to the oxidized products of alkyl carbonates. XPS measurements on the charged materials did reveal the presence of significant quantities of carbon-containing compounds and lithium fluoride on the surface of the charged electrode. The presence of LiF suggests that the $LiPF_6$ electrolyte salt was also unstable and decomposed under these conditions.

In view of the mechanism of electrochemical activity of Li_2MnO_3 described here there are at least two possible explanations for why the charge−discharge curve displays a plateau on the first charge. Either the ion exchange process involves a two-phase reaction or the rate-limiting step is oxidation of the electrolyte. In the latter case the chemical potentials of the species taking part in the redox reaction within the electrolyte are unlikely to change significantly with state-of-charge, and, assuming the reaction is not mass transport controlled, then a relatively invariant potential may be expected. We have examined powder X-ray diffraction patterns as a function of the state-of-charge (degree of ion exchange) on the first charge but we find little evidence for a two phase reaction until a sufficiently high degree of exchange has taken place for the formation of the P3 phase. Before this phase appears the peaks associated with the Li_2MnO_3 phase shift continuously as ion exchange proceeds. We therefore conclude that the plateau, which is already well developed before the appearance of the P3 phase, is most likely associated with the electrochemical generation of protons at the electrode surface.

Acknowledgment. P.G.B. is indebted to the Royal Society and the EPSRC for financial support. Dr. S. M. Francis and Professor N. V. Richardson (St. Andrews) are thanked for conducting the XPS measurements. Y. Paik and Professor C. P. Grey are thanked for conducting the ^{1}H NMR experiments.

Supporting Information Available: XPS data for the samples listed in Table 1 including data fits (PDF).

CM030047U

(38) Thomas, M. G. S. R.; Bruce, P. G.; Goodenough, J. B. *J. Electrochem. Soc.* **1985**, *132*, 1521.
(39) Aurbach, D.; Markovsky, B.; Levi, M. D.; Levi, E.; Schechter, A.; Moshkovich, M.; Cohen, Y. *J. Power Sources* **1999**, *81−82*, 95.
(40) Matsuo, Y.; Kostecki, R.; McLarnon, F. *J. Electrochem. Soc.* **2001**, *148*, 687.